



# Tracking Anterior Mitral Leaflet in Echocardiographic Videos Using Morphological Operators and Active Contours

Malik Saad Sultan<sup>1(✉)</sup>, Nelson Martins<sup>1,2</sup>, Eva Costa<sup>2</sup>, Diana Veiga<sup>2</sup>,  
Manuel João Ferreira<sup>2,3</sup>, Sandra Mattos<sup>4</sup>, and Miguel Tavares Coimbra<sup>1</sup>

<sup>1</sup> Instituto de Telecomunicações,  
Faculdade de Ciências da Universidade do Porto, Porto, Portugal  
{msultan,mcoimbra}@dcc.fc.up.pt

<sup>2</sup> Neadvance - Machine Vision, S.A., Braga, Portugal  
{nmartins,ecosta,dveiga,mferreira}@neadvance.com

<sup>3</sup> Centro Algoritmí, University of Minho, Guimarães, Portugal

<sup>4</sup> Círculo do Coração de Pernambuco, Recife, PE, Brazil  
ssmattos@cardiol.br

**Abstract.** Rheumatic heart disease is the result of damage to the heart valves, more often the mitral valve. The heart valves leaflets get inflamed, scarred and stretched which interrupts the normal blood flow, resulting into serious health condition. Measuring and quantifying clinically relevant features, like thickness, mobility and shape can help to analyze the functionality of the valve, identify early cases of disease and reduce the disease burden. To obtain these features, the first step is to automatically delineate the relevant structures, such as the anterior mitral valve leaflet, throughout the echocardiographic video. In this work, we proposed a near real time method to track the anterior mitral leaflet in ultrasound videos using the parasternal long axis view. The method is semi-automatic, requiring a manual delineation of the anterior mitral leaflet in the first frame of the video. The method uses mathematical morphological techniques to obtain the rough boundaries of the leaflet and are further refined by the localized active contour framework. The mobility of the leaflet was also obtained, providing us the base to analyze the functionality of the valve (opening and closing). The algorithm was tested on 67 videos with 6432 frames. It outperformed with respect to the time consumption (0.4s/frame), with the extended modified Hausdorff distance error of 3.7 pixels and the improved tracking performance (less failure).

**Keywords:** Ultrasound images · Medical image processing  
Active contours · Segmentation and tracking · Mitral valve

# 1 Introduction

## 1.1 Motivation

Mitral valve diseases are widespread and are commonly affected by Rheumatic Heart Disease (RHD) [1]. RHD is an autoimmune disease that usually begins in childhood. It starts as a strep throat infection that is caused by the streptococci. If the strep throat infection is untreated, it results into rheumatic fever. The repeated episodes of rheumatic fever slowly damages the heart valves.

Following one of the most relevant published studies [2, 3], about 15.6 million people are affected globally from RHD, and require medical follow-up, being responsible for 233,000 deaths per year. Heart valve diseases create a massive economic burden on health authorities. The average surgery cost to treat mitral regurgitation was  $24,871 \pm 13,940$  dollars per patient in Europe [4–6]. The heart valve treatments and operations are not only expensive, but also a highly risky cardiac process [7].

The literature suggests the cost effective solution of using penicillin in the early stage [8]. It reduces the probability of recurrence of the rheumatic fever, resulting less risk of damage to the heart valves. Therefore, earlier detection is considered vital to control disease progression and to estimate disease burden in low-resource regions of the world [1].

RHD thickened the Anterior Mitral Leaflet (AML) that directly affects the shape and mobility of the leaflet, resulting into pathologies like stenosis and regurgitation. Quantifying the degree of change in morphological features helps to identify early cases and to control disease progression.

The key benefits of using the Echocardiography modality are its non-ionizing, non-invasive property and is able to analyze fast moving structures like AML in real time. It is a low cost modality and is available as a portable device that makes it the most appropriate choice to use it in low resource areas [9].

The Parasternal Long Axis view provides the most suitable window to measure and quantify the clinically relevant parameters of the mitral valve such as, thickness, mobility and valvular anatomy (Fig. 1) [10]. To achieve this the first step is to segment and track the structures throughout the cardiac cycle. Manual segmentation is undesirable, given its impracticality, subjectivity and expert knowledge required. Automatic and semi-automatics methods to identify and track mitral valve structures can improve the diagnostic process, providing quick and objective measurements of clinically relevant parameters, even without any expert cardiology knowledge.

## 1.2 State of the Art

Active contour models were used to delineate the objects with deformable shapes and were extensively used by the research community for segmentation and tracking of the structures in medical images. The reason to adopt this kind of approach is their robustness against image noise and shape fragmentation, ability to track non-rigid motion and its capability to incorporate geometric

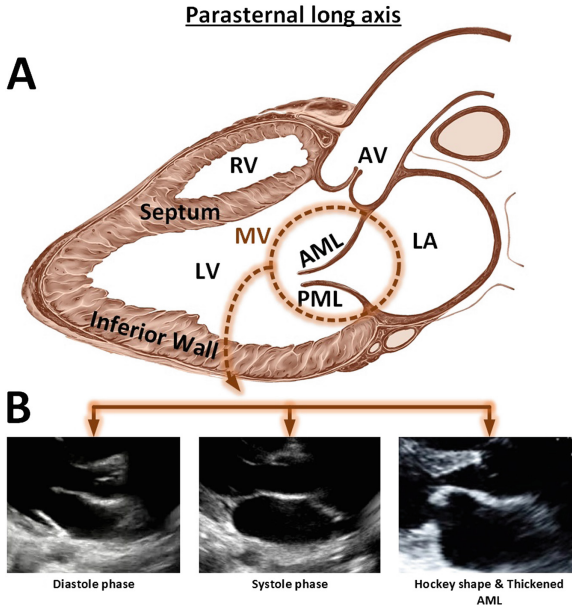


**Fig. 1.** Parasternal long axis view, (adapted from [24]) (A): showing Mitral valve (MV), Anterior Mitral Leaflet (AML), Posterior Mitral Leaflet (PML) and other structures. (B): Shows the MV in Diastole/Systole phase, the thickened and hockey shape leaflet.

constraints, such as the expected shape [11]. Optical flow was integrated in the active contour framework to segment and track the AML in echocardiography [12]. The limitations of the proposed method are, incapability to track large frame to frame displacement of AML, require manual initialization in the first frame and was computationally expensive to process a single cardiac cycle (20 m). In another work, transformation fitting was used to obtain initial boundaries that are further refined by the two connected active contours [13]. The proposed method requires initialization, parameter adjustment, failed in high displacement ( $\geq 10$  pixels) and is computationally expensive with 1.8 s/frame for the ten iterations. A fully automatic and unsupervised method was based on outlier detection in a low rank matrix to track the region of the AML, in both 2D and 3D ultrasound images [14]. Despite the fact that it is fully automatic, it is very sensitive rank and noise. Literature review demands a real time segmentation and tracking algorithm with less user interaction and the ability to efficiently track the mitral valve when faced with a large frame to frame displacements [11–14].

Mathematical morphology is widely used in image processing for analysis of shapes, geometrical and topological structures. They were previously used to segment the left ventricle [15], myocardium, ischemic viable and non-viable in echocardiography [16].

### 1.3 Objectives and Contributions

The objective of this work is to obtain robust and real-time tracking of the AML in ultrasound videos.

Our key contribution in this work is the novel use of combined morphological operators and active contours to address robust AML tracking in frames with large displacement.

The remainder of the paper is organized as follows. Section 2 provides the methodology adopted in this paper. In Sect. 3 we report the results that demonstrate the accuracy of the proposed algorithm and finally Sect. 4 concludes the paper with a discussion on the problem, our contribution to it and the future work.

## 2 Methodology

In the first step, echocardiography video is read, followed by contrast stretching to normalize the illumination of the image. In this work, we assumed the perfect segmentation (manual) in the first frame and is provided in priori. In each step, two successive frames are iteratively selected. Since AML is a thin region that shows fast motion, the thin regions of the successive images are extracted followed by the regions with large displacement, using basic mathematical morphological techniques. These regions are subsequently merged with the segmentation result of the preceding frame and filtered, in the candidate region module. Obtained regions are classified by taking into account their shapes and geometrical properties. The obtained boundaries of the AML with morphological operator are not well localized. Therefore localized active contour model is used to refine the obtained boundaries. After having the segmentation results, we proceed to the post processing step of AML analysis. A summary of the proposed processing pipeline is depicted in Fig. 2, and each step will now be discussed in detail.

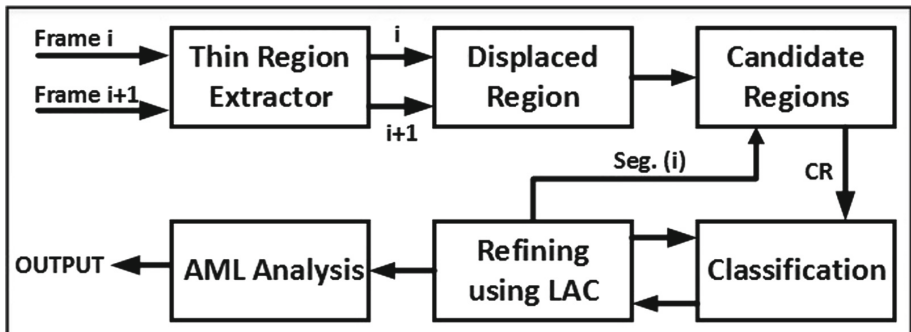


Fig. 2. AML tracking pipeline (adapted from [24]).

## 2.1 Thin Region Extractor

In this stage, two consecutive frames were extracted iteratively until the whole cardiac cycle was covered. The basic mathematical morphological operations were used that requires, the input image and the structuring element of suitable size and shape. These morphological operations can be used for both binary and grayscale images. For the resolution of the videos used in this papers experiments the maximum recorded thickness of the AML was 24 pixels. Following this, we used the grayscale images with the disk shape structuring element of width 24 pixels, to extract the potential regions.

Finally, The thin AML region (Fig. 3C) is extracted by taking the difference between the grayscale input image (Fig. 3A) and the grayscale opened image (Fig. 3B) with the flat disk shape structuring element of 24 pixel diameter.



**Fig. 3.** (A) Grayscale image (B) Morphological opening (C) Top-hat transform (adapted from [24]).

## 2.2 Displaced Region

Based on the analysis of the AML in the PLAX view, the thin AML region shows a very large displacement in successive frames, compare to other regions in an image. Other regions such as, septum, inferior wall (Fig. 1) do not show significant displacement in successive frames and thus the regions are overlapped. This prior information is meaningful to overcome the problem of tracking in frames with large AML displacement.

The focus of this module is to extract region that showed large displacement from frame  $t - 1$  to frame  $t$ . That can simply be achieved by taking the difference of successive frames followed by selecting only the positive intensity values (Fig. 4). Hard threshold is then applied to get the binary image.

$$Disp_{gray}^t = [I_t(x, y) - I_{t-1}(x, y)] \quad Disp_{gray}^t < 0 \quad (1)$$

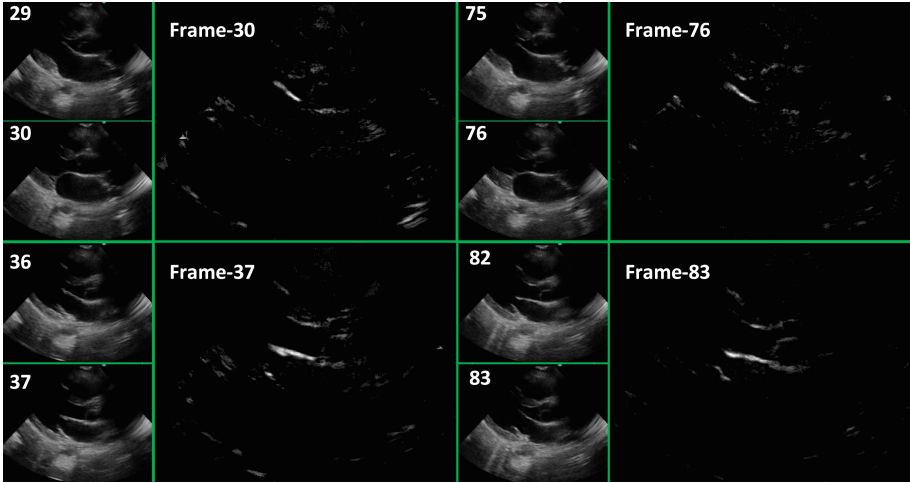


**Fig. 4.** Regions with high displacement at four different times (frames) (adapted from [24]).

### 2.3 Candidate Image

The segmented region obtained at the time  $t - 1$  is filtered to remove the regions which belong to the blood pool (black region) in frame at time  $t$ . The filtered region is then summed up with the results of the displaced region module. Small discontinuities (with a distance of 2 pixels or less) were merged by a morphological closing using a disk shape structuring element with a radius of 2. The obtained results are shown in Fig. 5.

### 2.4 Region Classification

The regions extracted from the last module are classified as the AML or the outliers, based on the morphological features such as area, centroid, minor axis length, major axis length. These features provides the structural and locality information to assign the probability of being the AML or outlier.

These basic morphological features do not typically change significantly in successive frames. In ideal conditions, these features should be constant throughout the cardiac cycle. The features obtained from the manual segmentation in the first frame is used as a reference for the upcoming frame. After processing each frame, the reference features are automatically updated with the average, by using the feedback channel (Fig. 6).

An error matrix is designed that compute the relative error compare to the segmentation in previous frames. The error matrix consist of four vectors, area error: computes the change in area, centroid error: computes the change in location, major/minor axis length error: computes the change in length and width. Next, the region with the minimum overall error is classified as the AML and other as outliers.

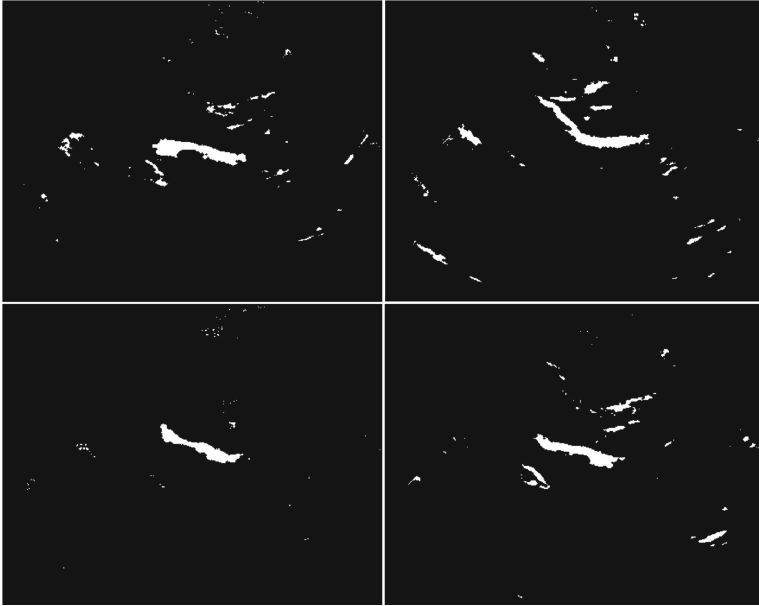


Fig. 5. Candidate image for final AML classification (adapted from [24]).

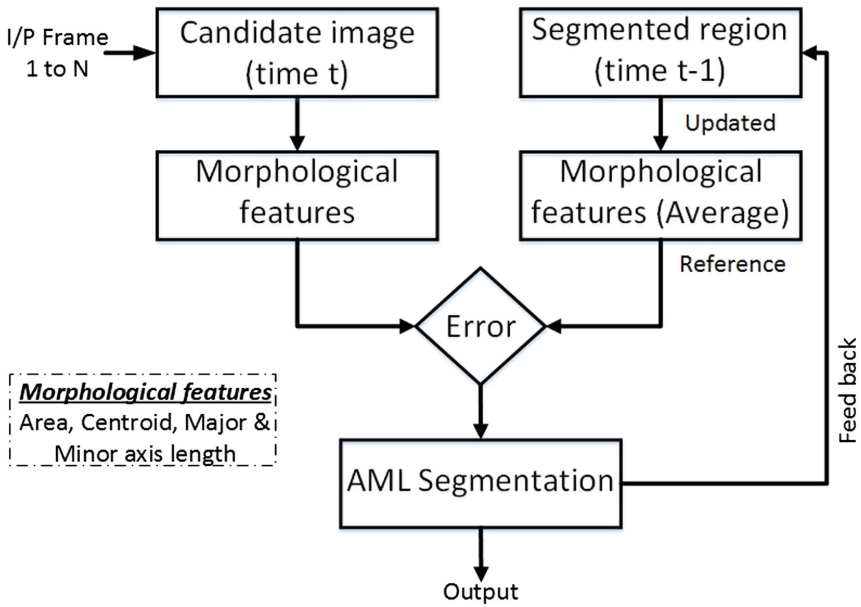


Fig. 6. Classification scheme (adapted from [24]).

## 2.5 Refining Using Active Contours

The active contour framework has been widely used for the purpose of image segmentation and tracking [17]. The contour deforms under the internal and external energy to segment the desired object. The active contours can be broadly divided as, the edge based and the region based [18, 19].

The edge based active contours [18] uses the image gradient (edges) to attract the contour towards the desired boundary. Active contour framework requires the placement of contour close to the object and is sensitive to the image noise. However, it work reasonably well in images with heterogeneous regions.

The region based active contours [19] uses the global intensity statistics of the regions to evolve the contour, until find the optimum choice. They are not sensitive to initial placement of the contour and is insensitive to noise.

**Automatic Initialization.** The boundaries of the AML obtained by the mathematical morphological techniques are used to initialize the active contour framework. Initial boundaries are close to the real boundaries, but are not well localized. Therefore, analyzing local regions can provide robust and well defined boundaries, with a few iterations.

**Localized Active Contours.** Ultrasound images are very noisy and frequently contain heterogeneous regions, and as such neither edge based contours, nor region based contours are a suitable choice. In this situation, we need a model that take the benefits from both edge and region based active contours. A localized region-based active contour (LAC) framework [20] were proposed to address this problem. This hybrid region-based curve evolution is robust to noise and doesn't rely on the global configuration of the image.

The rough boundaries of the AML obtained from the morphological operators were used to initialize the LAC framework, to refine the leaflet boundaries. The algorithm is based on the analysis of the local circular regions with five pixels radius, at each point on the curve. At each point the algorithm locally identifies the background and foreground optimally by their mean intensities. The formulation of the local energy function along the curve is defined as:

$$\begin{aligned} \frac{\partial \phi}{\partial t}(x) = & \delta \phi(x) \int_{\Omega_y} B(x, y) \delta \phi(y) \cdot ((I(y) - u_x)^2 \\ & - (I(y) - v_x)^2) dy + \lambda \delta \phi(x) \operatorname{div} \left[ \frac{\nabla \phi(x)}{|\nabla \phi(x)|} \right] \end{aligned} \quad (2)$$

Here,  $\delta$  is the Dirac function,  $B(x, y)$  represents a region that locally defines the interior and the exterior of the region at point  $x$  and the radius of the local region is specified by the user. The uniform modelling energy is used as an internal energy [19]. The localized version of the internal energy is defined as the local interior regions and exterior regions at each point on the curve.  $(v_x, \nu_x)$  are the localized version of means at each point  $x$ . The second term is the normalization term that keeps the curve smoother. It penalizes the arc length based on the weights  $\lambda$  tuned by the user.

## 2.6 AML Analysis

**Skeletonization.** Prior to perform the analysis, the shape of the AML is simplified by using skeletonization. The morphological thinning is used to get a line of one pixel width, while preserving the topological characteristics of the AML. Skeletonization works in the same way as morphological operators, convolving the structuring element (template) on the binary image. The Mark-and-Delete based templates were found very reliable and effective for thinning algorithms and thus used in this work [21]. Ultrasound images are usually affected by the speckle noise resulting into irregular boundaries, producing superfluous minor branches of the skeleton. These branches are filtered out to extract the fundamental part of the skeleton. This can be done by computing the Euclidian distance between the branch and the end points. All those branches whose length are less than the defined threshold (6 pixels) are discarded.

**Motion Patterns.** The focus of this module is to compute the motion pattern of the AML and analyze to extract the meaningful information. The mean motion of the X and Y coordinates of the skeleton was computed. The motion of the AML in X-axis was small and doesn't provide any meaningful information. However, the motion of the AML in Y-axis has shown large motion with a unique pattern. The mean of the y-coordinates of the AML skeleton for each frame is plotted against time, showing the motion pattern of the AML (Fig. 7). The cardiac cycle is divided into systole and diastole phase based on the maximum and minimum of the peaks of the obtained motion pattern. The classification helps to label the AML as open or close and will be useful for the analysis such as, computing the thickness when the valve is open. Further work can help to classify frames in early filling and late filling phase (Fig. 7). The late filling will be useful to extract frames in which the AML is perpendicular to the ultrasound beam. This is the best position to measure the thickness of the AML tip, which provides a strong clue regarding the presence or not of diseases.

**Shape.** The hockey stick like appearance of the AML in PLAX view is an indicator of stenosis. A condition in which the heart valve leaflets get restricted (narrowed, blocked) resulting into interruption in the normal blood flow. In order to identify this condition, we proposed the measurement of the local curvature on the skeleton of the AML. A template based method is used to measure the local bending of the AML [22]. We tested two template based methods, the trigonometrical and crossover point method (Fig. 8).

The trigonometrical approach relates the crossover angle with the curvature (Eq. 3). The crossover angle is the angle between the crossover point, where the curve intersect the disk mask and the X-axis of the disk. This approach is sensitive to noise to estimate the precise angle of the crossover points.

$$K_{tr} = \frac{2\sin\theta_c}{1 - \sin^2\theta_c} \quad (3)$$

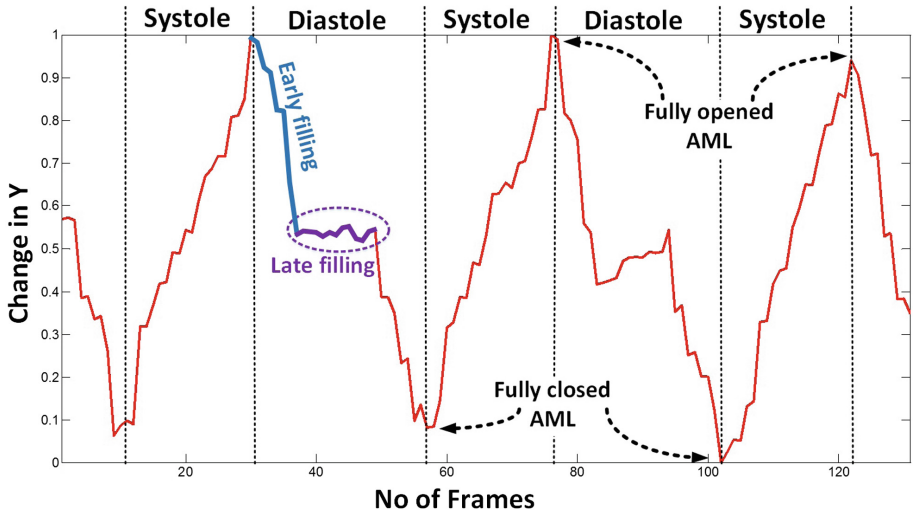


**Fig. 7.** Motion patterns generated by AML (adapted from [24]).

The crossover point approach approximate the curvature by computing the area between curve and the disk, and is related to the crossover angle ( $\theta_c$ ) [22]. The squared area covered by the curve and disk are inversely proportional to the curvature (Eq. 4).

$$K_{cp} = \frac{1}{A^2} \quad (4)$$

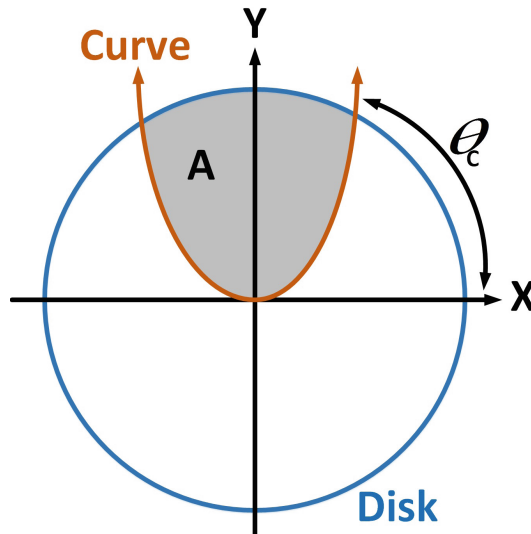


**Fig. 8.** Curvature approximation using area and crossover angle  $\theta_c$ .

The obtained area is large for the small curvature. Thus the reciprocal of squared area is close to zero that increase the confidence by avoiding infinity and the reliability of the approach.

The experiments has shown that the area based method is less sensitive to speckle noise and provide smoother results, and thus used for this analysis. For each frame, we measured the local curvature at each point on the AML skeleton, followed by computing the overall mean to obtain the global curvature. In stenosis, the leaflet is restricted and can be identified by the curvature (shape) change.

We observed that the motion pattern of the AML and the pattern of the global curvature change are correlated. When the valve opens the curvature of the AML tends to decrease showing the straightness of the leaflet and when the valve opens the curvature start increasing, suggesting the bending of the leaflet. This motion shape relation might help in future by providing a clue to identify pathological condition.

For a better visual representation of the motion and curvature pattern, we first smoothed the curved and then normalize to restrict it in the range (0–1) (Fig. 9).

## 3 Results

### 3.1 Materials

An initiative from the Real Hospital Português, in Recife, Brazil lead to the screening of 1203 childrens and pregnant women, looking for cardiac pathologies. All patients were tested regarding the presence of streptococcal infection and short mitral valve videos were recorded. The data were collected using different ultrasound devices (M-Turbo, Edge II model by SonoSite, Vivid my model

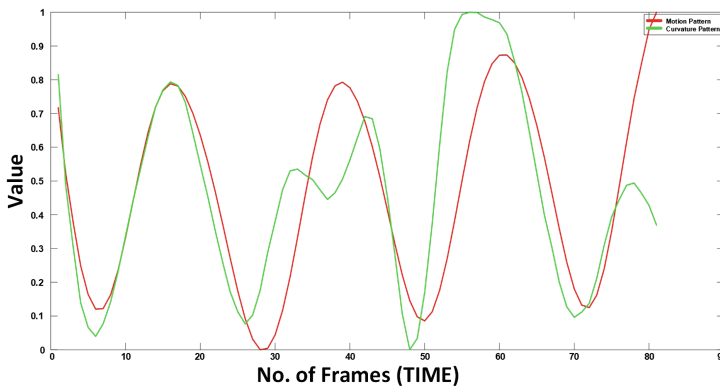


**Fig. 9.** Motion and curvature pattern of AML, red: motion pattern, green: curvature pattern. (Color figure online)

by *GE* healthcare and *CX50* model by Philips), with a wide range of transducers, frequency and scanning depths. Sixty seven of these exams was manually annotated by the doctors using *Osirix* software and were used to test the novel method proposed in this work. These sixty seven videos include a total of 6432 frames with a dimensions of  $422 \times 636$  pixels. The proposed method has been implemented using *MATLAB* R2016b.

### 3.2 Extended Modified Hausdorff Distance (E-MHD)

The Modified Hausdorff Distance [23] was proposed to obtain a distance measure to match two objects. In this work, we extended this approach by categorizing the segmented region as false positive, false negative and true positive. We assumed that the nearest point between Automatic Segmentation (AS) and Ground Truth (GT) with Euclidean distance smaller than 2 pixels are true positives. The part of the AS that is falsely segmented as AML were considered false positives and the parts of the GT that were missed by the automatic segmentation were considered as false negatives, always using 2 pixels distance as reference T (Fig. 10).

$$\begin{aligned} d_{AS \rightarrow GT} &= \min \{AS, SEG\} \quad FP = d > T \quad TP = d < T \\ d_{GT \rightarrow AS} &= \min \{AS, SEG\} \quad FN = d > T \quad TP = d < T \\ D_{MHD} &= \max [avg (d_{AS \rightarrow GT}), avg (d_{GT \rightarrow AS})] \end{aligned} \quad (5)$$

### 3.3 Segmentation and Tracking

In this section, we analyze and compare the tracking ability of the proposed algorithm on 67 cases in 2D ultrasound videos, obtained from the PLAX view. To validate the algorithm, we compared the results of the proposed algorithm with the doctors annotation. Results were also compared with the reference state of the art algorithm [25]. The reference algorithm used the modified internal energy

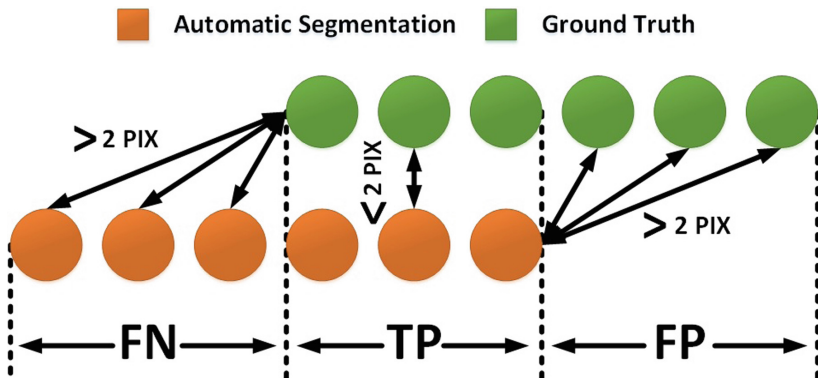


Fig. 10. Region classification (adapted from [24]). (Color figure online)

(open-ended contour) and external energy (added Harris cornerness measure), to track the AML in ultrasound. We used the E-MHD error to compute the relative Euclidean distance between AS and GT.

In this work, we assumed perfect segmentation (manual annotation) in the very first frame of the video, followed by defining the region of interest. It helps to removes the irrelevant structures from the right and left of the AML.

### 3.4 Quantification

The performance metric used are: the E-MHD error, the number of failures and the processing time. The morphological operators are relatively fast to obtain the boundaries of the AML, spending on average 0.4 s/frame, however the reference algorithm consumes 1.2sec/frame. To refine the obtained boundaries, we used the LAC that consumes about 0.7 s/frame. The boxplot is used for the statistical analysis of the mean E-MHD and the number of failure in each video. The E-MHD error was computed for each frame of the video and the mean E-MHD error was saved in a vector for visual inspection.

The boxplot of E-MHD error (Fig. 11) shows that the median E-MHD error of our method is smaller than the reference algorithm, 3.7 and pixels 5.2 respectively. The most frequent error for our method lies between 3.14 to 4.6 pixels. However, the reference algorithm covers the comparatively large range from 4.6 to 6.6 pixels. The overall range of our method is also improved, from 2.12 to 5.54, whereas the reference covers the higher values from 3.32 to 8.06 pixels. In the Fig. 10, the red dots shows the outliers.

Proposed method has shown an improvement in tracking, with a median number of failure in each video of 2 (Fig. 12). The reference method failed twice as much than proposed method (median of 4). The most frequent range of failure

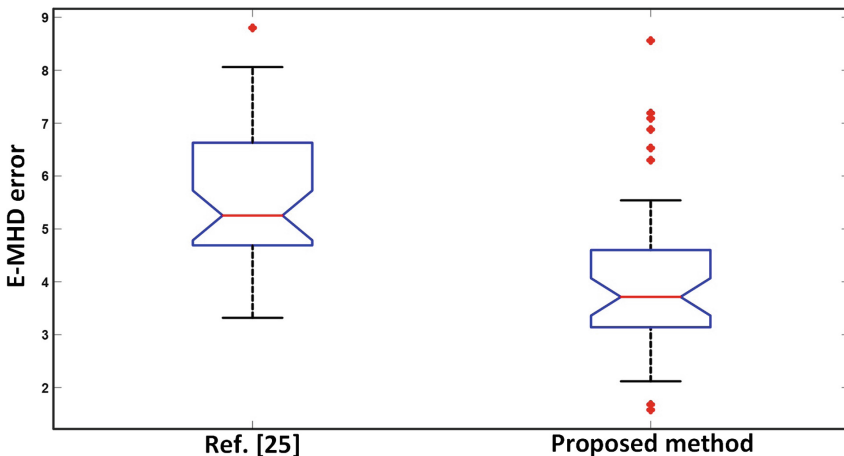
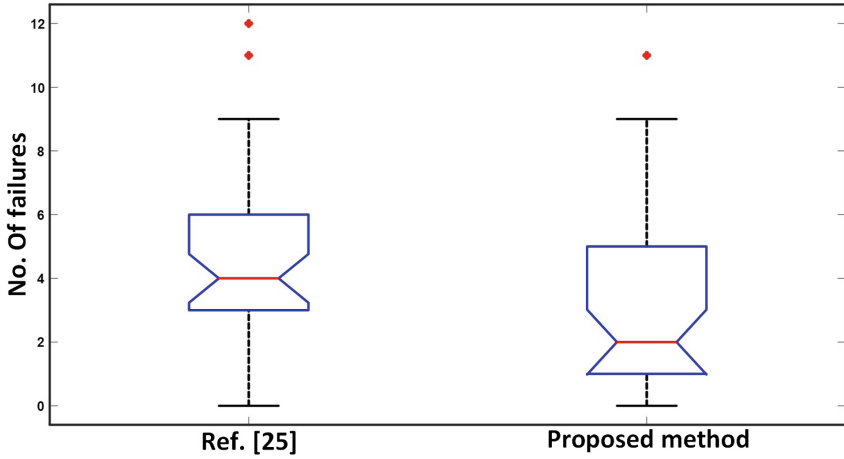


Fig. 11. Extended modified Hausdorff distance error, 67 cases.



**Fig. 12.** Number of failure in each video, 67 cases.

in proposed method is between 1 to 5 failures. On the other side, the reference method shows lies between 3 to 6 failures.

Proposed algorithm has performed reasonably well, with respect to time consumption, E-MHD and the number of failures. The limitation of the work are the incapability of the algorithm to avoid segmenting the neighbor regions. The algorithm is robust to segment the whole leaflet with a sensitivity of 85% and a recall of 72%.

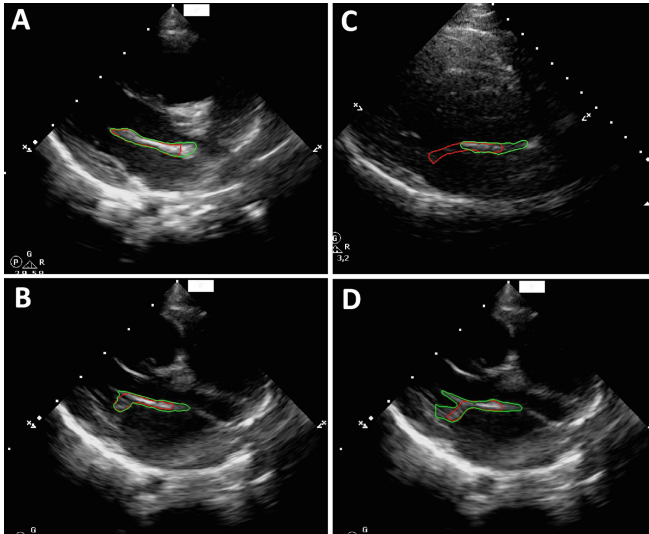


**Fig. 13.** Segmentation results, red: doctors's annotation, green: proposed method. (Color figure online)

The segmentation results were plotted for better problem understanding. The Fig. 13A, B shows the reasonable results with fully segmented AML and with the small region falsely segmented as the AML. However, in Fig. 13C we have the discrete regions in an image and thus missed by the proposed algorithm and is one of the reason, why the proposed method fails. In Fig. 13D, the proposed method has segmented not only the AML, but also segmented the chordae tendineae and the posterior aorta. These missing and over-segmented regions are the responsible of having large E-MHD, with low sensitivity and recall.

## 4 Discussion and Future Work

In this work, a new tracking approach is proposed that uses morphological operators to predict the location and boundaries of the AML. To obtain more precise boundaries, the localized active contour framework is adopted. The algorithm is found robust to track in the difficult situations when the valve opens with the mean AML displacement of about 35 pixels. In such situation, the active contours often fails to segment the boundaries (edges) that are far from the contour. The proposed algorithm outperform the reference algorithm with respect to time, however it is still slow to get the real time performance of the algorithm.

The main limitation of the algorithm is its incapability to avoid segmenting the neighbor regions (chordae tendineae, cardiac walls, septum etc.). It happens because the intensity and texture of the neighbor regions are similar. The chordae tendineae and the posterior aorta are directly connected with the AML, containing the same features. So we dont have any reliable feature that identify starting and ending of the leaflet. In this work, we define the region of interest that minimize this problem, however we need an automatic system that robustly define the region of interest and impose the shape constraints in the active contour frame work to further improve the segmentation performance.

Another limitation of the proposed algorithm is its incapability to recover from the failure. This is the situation that occur frequently due to low quality of the image and due to the missing structures in several frame of the ultrasound video.

In future, we will focus to overcome the limitations such as, the time consumption, reduce failure, minimize segmenting irrelevant regions, and finally to estimate and quantify morphological features to identify pathological cases.

**Acknowledgements.** This article is a result of the project NORTE-01-0247-FEDER-003507-RHDecho, co-funded by Norte Portugal Regional Operational Programme (NORTE 2020), under the PORTUGAL 2020 Partnership Agreement, through the European Regional Development Fund (ERDF). This work also had the collaboration of the Fundação para a Ciência e Tecnologia (FCT) grant no: PD/BD/105761/2014 and has contributions from the project NanoSTIMA, NORTE-01-0145-FEDER-000016, supported by Norte Portugal Regional Operational Programme (NORTE 2020), through Portugal 2020 and the European Regional Development Fund (ERDF).

## References

1. Bisno, A., Butchart, E.G., Ganguly, N.K., Ghebrehiwet, T., et al.: WHO Expert Consultation on Rheumatic Fever and Rheumatic Heart Disease, Geneva (2004)
2. WHO: World Heart Federation, World Stroke Organization. Global atlas on cardiovascular disease prevention and control (2011). ISBN 9789241564373
3. WHF (2012). [http://www.world-heart-federation.org/fileadmin/user\\_upload/documents/Fact\\_sheets/2012/RHD.pdf](http://www.world-heart-federation.org/fileadmin/user_upload/documents/Fact_sheets/2012/RHD.pdf)
4. Trochu, J.N., Tourneau, T.L., Obadia, J.F., Caranhac, G., Beresniak, A.: Economic burden of functional and organic mitral valve regurgitation. *Arch. Cardiovasc. Dis.* **108**, 88–96 (2015)
5. Ribeiro, G.S., Tartof, S.Y., Oliveira, D.W.S., Guedes, A.C.S., Reis, M.G., Riley, L.W., Ko, A.I.: Surgery for valvular heart disease: a population-based study in a Brazilian urban center. *PLoS One* **7**(5), e37855 (2012)
6. The economic cost of cardiovascular disease from 2014–2020 in six European economies. Centre for Economics and Business Research, London (2014)
7. Mirabel, M., Iung, B., Baron, G., Messika-Zeitoun, D., Dtaint, D., Vanoverschelde, J.-L., Butchart, E.G., Ravaud, P., Vahanian, A.: What are the characteristics of patients with severe, symptomatic, mitral regurgitation who are denied surgery? *Eur. Heart J.* **28**, 1358–1365 (2007)
8. Colquhoun, S.M., Carapetis, J.R., Kado, J.H., Steer, A.C.: Rheumatic heart disease and its control in the Pacific. *Expert Rev. Cardiovasc. Ther.* **7**(12), 1517–1524 (2009)
9. Remnyi, B., Wilson, N., Steer, A., Ferreira, B., Kado, J., Kumar, K., Lawrenson, J., Maguire, G., Marijon, E., et al.: World Heart Federation criteria for echocardiographic diagnosis of rheumatic heart diseasean evidence-based guideline. *Nat. Rev. Cardiol.* **9**(5), 297–309 (2012)
10. Omran, A.S., Arifi, A.A., Mohamed, A.A.: Echocardiography of the mitral valve. *J. Saudi Heart Assoc.* **22**, 165–170 (2010)
11. Sheng, C.: Segmentation in echocardiographic sequences using shape-based snake model. *Comput. Inf.* **27**, 423–435 (2008)
12. Mikic, I., Krucinski, S., Thomas, J.D.: Segmentation and tracking in echocardiographic sequences: active contours guided by optical flow estimates. *IEEE Trans. Med. Imaging* **17**(2), 274–284 (1998)
13. Martin, S., Daanen, V., Chavanon, O., Troccaz, J.: Fast segmentation of the mitral valve leaflet in echocardiography. In: Beichel, R.R., Sonka, M. (eds.) CVAMIA 2006. LNCS, vol. 4241, pp. 225–235. Springer, Heidelberg (2006). [https://doi.org/10.1007/11889762\\_20](https://doi.org/10.1007/11889762_20)
14. Zhou, X., Yang, C., Yu, W.: Automatic mitral leaflet tracking in echocardiography by outlier detection in the low-rank representation. In: IEEE Conference on Computer Vision and Pattern Recognition, pp. 972–979. IEEE Computer Society, Washington, DC (2012)
15. Yun-gang, L., Jacky, K.K., Shi, L., Guan, Y., Linong, L., Qin, J., PhengAnn, H., Winnie, C.C., Defeng, W.: Myocardial iron loading assessment by automatic left ventricle segmentation with morphological operations and geodesic active contour on T2\* images, Scientific reports (2015)
16. Lascu, M., Lascu, D.: A new morphological image segmentation with application in 3D echographic images. *WSEAS Trans. Electron.* **5**(3), 72–82 (2008)
17. Noble, J.A., Boukerroui, D.: Ultrasound image segmentation: a survey. *IEEE Trans. Med. Imaging* **25**(8), 987–1010 (2006)

18. Kass, M., Witkin, A., Terzopoulouse, D.: Snakes : active contour model. *Int. J. Comput. Vis.* **1**(4), 321–331 (1988)
19. Chan, T., Vese, L.: An active contour model without edges. In: Nielsen, M., Johansen, P., Olsen, O.F., Weickert, J. (eds.) *Scale-Space 1999*. LNCS, vol. 1682, pp. 141–151. Springer, Heidelberg (1999). [https://doi.org/10.1007/3-540-48236-9\\_13](https://doi.org/10.1007/3-540-48236-9_13)
20. Lankton, S., Tannenbaum, A.: Localizing region-based active contours. *IEEE Trans. Image Process.* **17**(11), 2029–2039 (2008)
21. Zhang, T.Y., Suen, C.Y.: A fast parallel algorithm for thinning digital patterns. *Commun. ACM* **27**(3), 236–239 (1984)
22. Masoud, A.S., Pourreza, H.R.: A novel curvature-based algorithm for automatic grading of retinal blood vessel tortuosity. *IEEE J-BHI* **20**(2), 586–595 (2016)
23. Dubuisson, M.-P., Jain, A.K.: A Modified hausdorff distance for object matching. In: *Proceedings of International Conference on Pattern Recognition*, Jerusalem, Israel, pp. 566–568 (1994)
24. Sultan, M.S., Martins, N., Costa, E., Veiga, D., Ferreira, M., Mattos, S., Coimbra, M.: Real-time anterior mitral leaflet tracking using morphological operators and active contours. In: *Proceedings of International Joint Conference on Biomedical Engineering Systems and Technologies*, Porto, Portugal (2017)
25. Sultan, M.S., Martins, N., Veiga, D., Ferreira, M.J., Coimbra, M.T.: Tracking of the anterior mitral leaflet in echocardiographic sequences using active contours. In: *EMBC*, pp. 1074–1077 (2016)